Molecular Therapy
Methods & Clinical Development
Original Article

Evaluation of the human type 3 adenoviral dodecahedron as a vector to target acute myeloid leukemia

Benjamin Caulier,[1,2,3] Gaëlle Stofleth,[2,4] Dalil Hannani,[1] Mélanie Guidetti,[3] Véronique Josserand,[3] David Laurin,[3,5] Jadwiga Chroboczek,[1] Pascal Mossuz,[2,3] and Dominique Plantaz[4]

[1]University Grenoble Alpes, CNRS, CHU Grenoble Alpes, Grenoble INP, TIMC-IMAG, 38000 Grenoble, France; [2]Institute of Biology and Pathology, Laboratory of Cellular Hematology, University Grenoble Alpes Hospital, Grenoble, France; [3]Institute for Advanced Biosciences, INSERM U1209, CNRS UMR 5309, University Grenoble Alpes, Grenoble, France; [4]Department of Pediatric Onco-Immuno-Hematology, University Grenoble Alpes Hospital, Grenoble, France; [5]Etablissement Français du Sang Auvergne Rhône-Alpes, Grenoble, France

Intensive systemic chemotherapy is the gold standard of acute myeloid leukemia (AML) treatment and is associated with considerable off-target toxicities. Safer and targeted delivery systems are thus urgently needed. In this study, we evaluated a virus-like particle derived from the human type 3 adenovirus, called the adenoviral dodecahedron (Dd) to target AML cells. The vectorization of leukemic cells was proved very effective at nanomolar concentrations in a time- and dose-dependent manner, without vector toxicity. The internalization involved clathrin-mediated energy-dependent endocytosis and strongly correlated with the expression of $\alpha_V\beta_3$ integrin. The treatment of healthy donor peripheral blood mononuclear cells showed a preferential targeting of monocytes compared to lymphocytes and granulocytes. Similarly, monocytes but also AML blasts were the best-vectorized populations in patients while acute lymphoid leukemia blasts were less efficiently targeted. Importantly, AML leukemic stem cells (LSCs) could be addressed. Finally, Dd reached peripheral monocytes and bone marrow hematopoietic stem and progenitor cells following intravenous injection in mice, without excessive spreading in other organs. These findings reveal Dd as a promising myeloid vector especially for therapeutic purposes in AML blasts, LSCs, and progenitor cells.

INTRODUCTION

Acute myeloid leukemia (AML) has one of the lowest survival rates among childhood cancers with a 5-year prognostic survival of 60% to 75%.[1,2] In adults, AML is the most common leukemia and patients under 60 years of age have a 5-year prognostic survival of 30% to 40% and this dramatically decreases below 15% above 60 years of age.[3] For decades, AML was classified according to cell morphology using the French-British-American (FAB) classification (AML M0 to M7, i.e., M3 acute promyelocytic leukemia). Since then, multiple revisions from the World Health Organization (WHO) led to 4 new classes: AML with recurrent genetic abnormalities, AML with myelodysplasia-related changes, therapy-related AML, and AML not otherwise specified.[4]

Although tremendous progress has been achieved over the past 40 years in the understanding of AML physiopathology, treatment has not substantially changed. Indeed, cytarabine and anthracyclines drugs, both impeding DNA replication, remain the gold standard of intensive chemotherapy treatment used in combination with hematopoietic stem cell (HSCs) transplantation but are associated with severe off-target toxicities and long-term sequelae, especially in children and elderly patients.[2,5–7] The specific targeting of AML cells is thus an important challenge to enhance overall chemotherapy tolerability, as well as for the delivery of new therapies.[8]

So far, many synthetic or bioinspired drug carriers are currently in development and trials but only few of them are in use with the most represented being liposomes and polymeric nanoparticles.[8,9] These carriers improve bioavailability and toxicity and may ameliorate remission. For example, Vyxeos, a liposomal formulation of cytarabine and daunorubicin in a 5:1 molar ratio, was approved by the FDA in 2017 and the EMA in 2018 for the treatment of adults with newly diagnosed high-risk secondary AML.[10,11] Among bio-inspired delivery systems, virus-like particles (VLPs) are stable, self-assembled homogeneous nanoparticles composed of virus capsid or envelope proteins.[12] They are easily producible, carry no genetic material, and represent a versatile tool for biomedical applications including cargo delivery for therapy.[13]

The capsid surface of the human serotype 3 adenovirus (Ad3) is composed of 3 structural proteins: the hexon, the fiber, and the penton base (Pb). The hexon is the major building block of adenoviruses capsid but also the most immunogenic protein responsible for the bulk of neutralizing antibody production,[14] especially against

Received 10 June 2020; accepted 10 November 2020;
https://doi.org/10.1016/j.omtm.2020.11.009.

Correspondence: Benjamin Caulier, PhD, Institute of Biology and Pathology, Laboratory of Cellular Hematology, University Grenoble Alpes Hospital, Grenoble, France.
E-mail: benjamin.caulier@gmail.com

the hypervariable loops that differ among adenovirus serotypes.[15] The Ad3 fiber directs targeting properties through its specific attachment to cellular receptors such as ubiquitous complement regulatory protein CD46,[16] epithelial desmoglein-2,[17] and costimulatory molecules CD80/86.[18] The Ad3 Pb is meanwhile responsible for the entry through the interaction of its RGD (Arg-Gly-Asp) motifs within $\alpha_V\beta_3$ and $\alpha_V\beta_5$ integrins present on cell membranes, which subsequently triggers endocytosis.[19–21] In addition, an important feature of Ad3 (but not Ad2 or Ad5) is its ability to produce dodecahedral VLPs during infection, consisting of fiber and Pb.[22] Otherwise, the recombinant expression of Ad3 Pb alone is sufficient to give rise to fiberless dodecahedron (Dd, commonly referred as Base [Bs]-Dd).[23,24] This simplified VLP is ~30 nm in diameter and is exclusively composed of 12 copies of Ad3 Pb. Similarly to the Ad3 of origin, Dd shares the entry mechanism connecting Pbs to α_V integrins.[25] Therefore, this VLP has been efficiently used in the delivery of proteins,[26,27] therapeutic compounds,[28] and mRNA analogs.[29] Recently, a study on human healthy blood demonstrated Dd natural affinity for leukocytes, ~45-fold higher than for red blood cells (RBCs) or platelets.[30]

We postulate that Dd can represent a promising vector for AML cells. We thus characterized its ability to target leukemic cells *in vitro* with attention for vector dose, subcellular localization, intracellular vector maintenance, endocytosis pathway, and toxicity. We compared the internalization among peripheral blood mononuclear cells (PBMCs) in healthy and patient settings with a focus on cell type targeting. Further, we assessed AML and acute lymphoid leukemia (ALL) blasts targeting, as well as the addressing of AML leukemic stem cells (LSCs) *ex vivo*. Finally, we evaluated the *in vivo* biodistribution of Dd following intravenous (i.v.) injection, especially in peripheral blood and bone marrow.

RESULTS

Dd efficiently vectorizes human leukemic cell lines

Dodecahedral VLPs were produced upon recombinant Ad3 Pbs expression in baculovirus-infected insect cells and purified by a two-step chromatography yielding soluble and stable nanoparticles (Figure S1; Supplemental Methods).

In this study, we first evaluated the vectorization of leukemic cell lines during 1 h with a labeled Dd (Dd-AF647). A significant increase of the percentage of Dd-AF647-positive cells was observed between 0.1 nM and 1 nM with a mean of 22% ± 18% and 94% ± 9%, respectively (Figure 1A). At 5 nM Dd, that percentage was over 98% for all cell lines. In addition, the relative amount of vector in cells (mean fluorescence intensity [MFI]) rose concomitantly with increasing concentration above 0.1 nM. The MFI signal increased over incubation time (Figure 1B) until 24 h ($p < 0.05$), and showed only a slow decline over 72 h indicating a good internal maintenance of the AF647 cargo (Figure 1C).

The vector toxicity was assessed over a week with treatment every 48 h (Figure 1D). We used 1 μM of doxorubicin as a positive cell death control (10 nM of doxorubicin had no effect; data not shown) since it induced 85.7% ± 7.8% of dead cells in 24 h (data not shown). A metabolic assessment of the viability indicated that 1, 5, and 10 nM Dd had a minor toxic effect with 93.6% ± 7.4%, 84.4% ± 14.3%, and 83.1% ± 13.9% of alive cells at day 7, respectively. Higher doses of 25 and 50 nM displayed much more toxicity, with 76.3% ± 11.5% ($p < 0.001$) and 55.7% ± 20.1% ($p < 0.0001$) of alive cells at day 7.

Of note, the AML cells displayed high intracytoplasmic content of particles often close to the nucleus, which was not assigned to membrane adsorption of Dd (Figure 1E).

Taken together, these results demonstrate Dd as a dose- and time-dependent vector, efficiently targeting leukemic cell lines while displaying moderate toxicity.

The Dd vectorization involves clathrin-mediated energy-dependent endocytosis and strongly correlates with $\alpha_V\beta_3$ integrin expression in leukemic cells

We investigated the effect of temperature and ATP depletion on the cellular uptake of Dd-AF647 in leukemic cells. The vector accumulation was reduced upon treatment at 4°C, with 87% of reduction in Dd-AF647 MFI compared to 37°C ($p < 0.01$; Figure 2A). Similarly, when the cellular ATP pool was depleted by treatment with sodium azide and 2-deoxy-D-glucose, the vectorization was nearly abolished with 96% of reduction ($p < 0.01$). These results indicated that the vectorization is temperature- and energy-dependent.

To clarify which endocytosis pathways is involved in leukemic cells vectorization, we explored the effect of wortmannin, methyl-β-cyclodextrin (MBCD), and chlorpromazine that specifically inhibit micropinocytosis/phagocytosis, caveolae/raft-, and clathrin-mediated endocytosis (CME).[31–33] When cells were treated with wortmannin or MBCD, Dd-AF647 MFI slightly decreased while the treatment with chlorpromazine significantly reduced Dd uptake of ~92% compared to control ($p < 0.05$; Figure 2B). Noteworthily, phagocytic Mono-mac-6 and THP-1 cells, as well as the chronic myeloid leukemia K-562, were less efficiently vectorized compared to others. These inhibition results showed that the active transport of Dd is carried out by CME.

Among integrins, $\alpha_V\beta_3$ is characterized as the entry receptor for Dd.[25] Therefore, we quantified its expression along Dd-AF647 internalization on leukemic cells. As expected, the MFI displayed a very close linear correlation between $\alpha_V\beta_3$ expression and the cellular level of Dd (Figure 2C). Conversely, although Dd was shown to interact with heparan sulfates,[34] a competitive inhibition of entry using heparin did not reduce Dd uptake in leukemic cells (Figure S2).

Taken together, these results reveal the leukemic cells Dd-mediated vectorization as a temperature- and energy-dependent phenomenon involving CME in $\alpha_V\beta_3$ integrin-expressing cells.

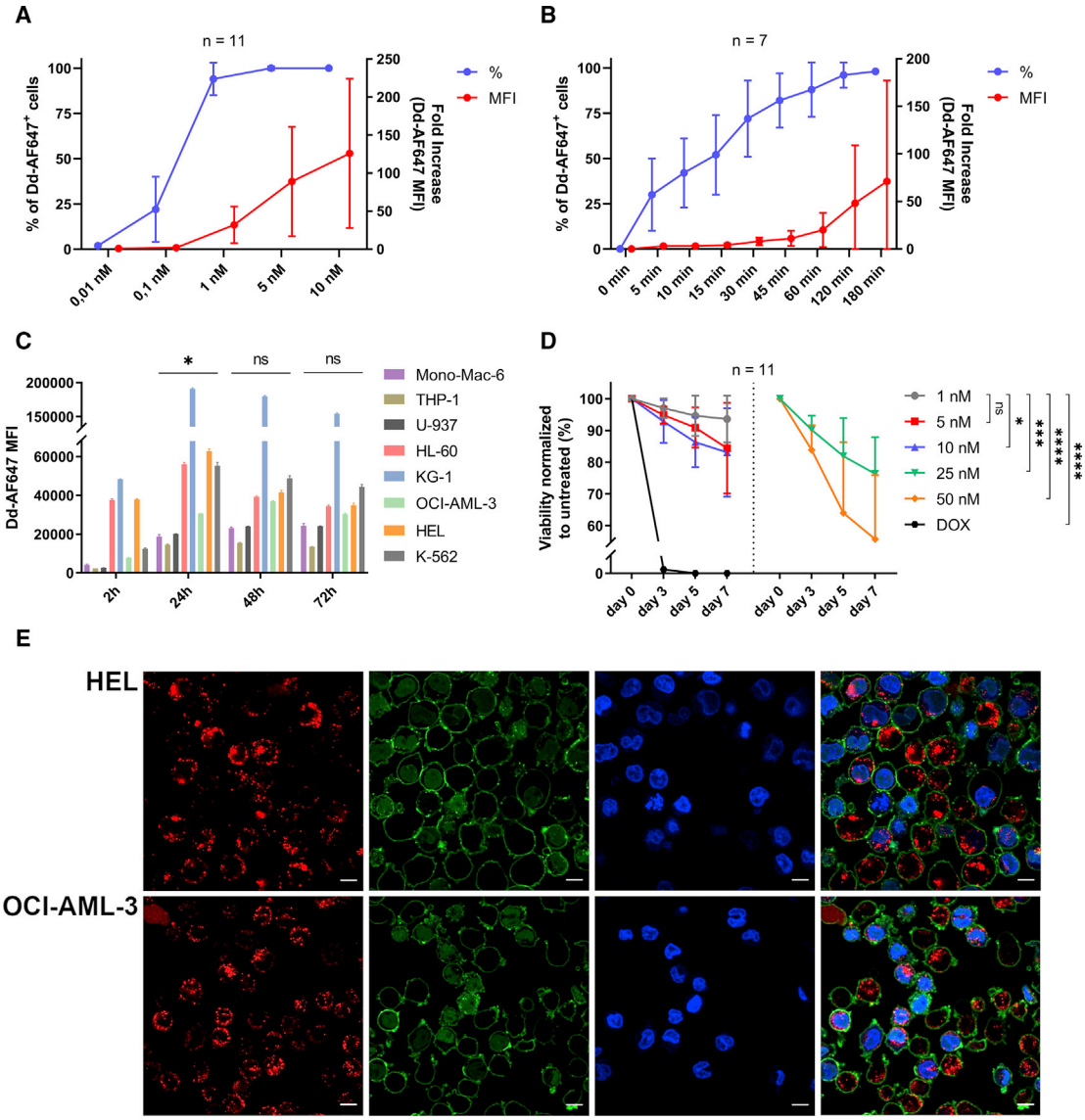

Figure 1. The adenoviral Dd efficiently vectorizes human leukemic cells, displaying robust intracellular maintenance and low toxicity

KG-1a, THP-1, Mono-Mac-6, SupB15, KG-1, OCI-AML-3, HEL, K-562, Jurkat, U-937, and HL-60 cells were incubated with Dd-AF647. The corresponding untreated cells were used as negative control. All measures were done in triplicates for each cell lines and the mean ± SD is indicated. p values were determined by one-way ANOVA (C) or two-way ANOVA (D). n.s., not significant; *$p \leq 0.05$; **$p \leq 0.01$; ***$p \leq 0.001$; ****$p < 0.0001$. (A) Effect of Dd concentration on the 11 cell lines during 1 h. In blue, cells positive (%) for Dd-AF647. In red, fold increase in Dd-AF647 MFI compared to untreated. (B) Effect of incubation time. KG-1a, THP-1, Mono-Mac-6, SupB15, KG-1, OCI-AML-3, and Jurkat were treated with 1 nM Dd-AF647 up to 180 min. (C) Persistence of Dd-AF647 inside treated cells. Cells were treated with 1 nM Dd-AF647 and analyzed at 2, 24, 48, and 72 h for AF647 MFI. (D) Effect of Dd on cell viability. The 11 cell lines were treated with repetitive doses of unlabeled-Dd every 24 h and assessed for viability by measurement of cell metabolism at days 0, 3, 5, and 7. Doxorubicin (DOX; 1 μM) was used as a cell death control. Left panel: DOX, 1, 5, and 10 nM Dd. Right panel: 25 and 50 nM Dd. (E) Cellular localization of Dd. HEL and OCI-AML-3 cells were incubated with 10 nM Dd-AF647 (red signal) during 2 h. Membranes were labeled with AF555-conjugated wheat germ agglutinin (green signal) and nuclei counterstained with DAPI (blue signal). Visualization was performed on a Zeiss LSM710 NLO microscope with a 63×/1.4 oil-immersion objective. Signals were collected after sequential laser excitation onto optical sectioning of 1 μm. Scale bars represent 10 μm.

Dd vectorizes human healthy donor peripheral blood mononuclear cells, preferentially targeting monocytes

PBMCs were purified from 25 healthy donor bloods and treated with Dd-AF647. Monocytes appeared as the best-targeted cells followed by B lymphocytes with 96% ± 4% and 47.7% ± 13.4% of Dd-AF647-positive cells for 1 nM, respectively ($p < .0001$, Figure 3A, left panel). Comparatively, granulocytes, T lymphocytes, and natural killer (NK) lymphocytes exhibited very close Dd penetration and were less efficiently vectorized. Importantly, T lymphocytes appeared to be the least-vectorized population, with 53.5% ± 6.7% of vector-positive cells

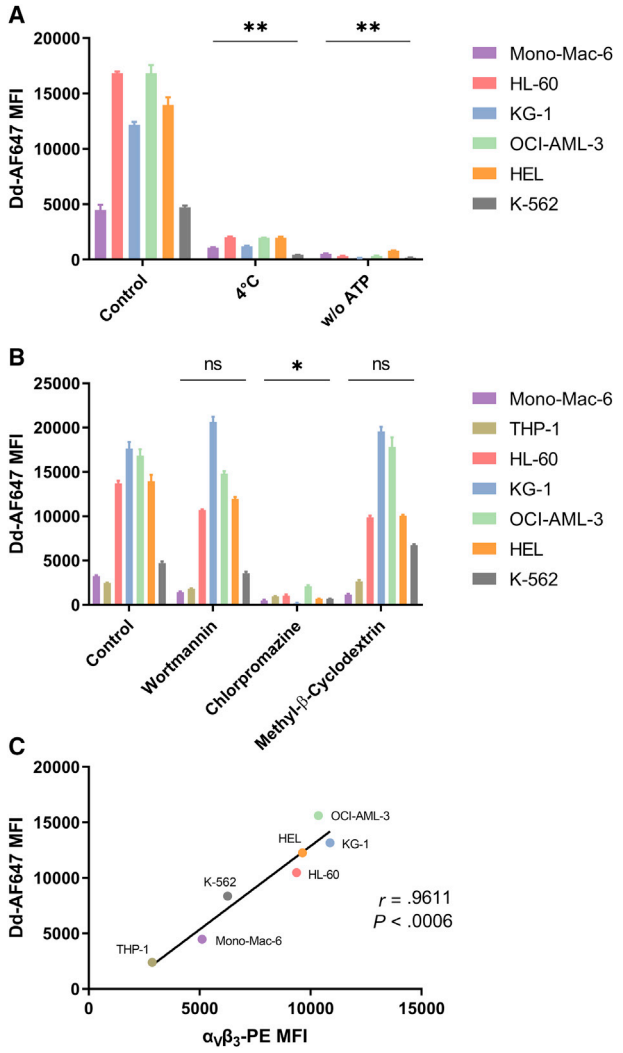

Figure 2. The vectorization is an energy-dependent phenomenon, involving clathrin-coated pit-mediated endocytosis and strongly correlating with $\alpha_V\beta_3$ integrin highly expressing cells

Leukemic cell lines were either pre-incubated at 4°C or with inhibitor drugs at 37°C in complete medium during 1 h before incubation with 1 nM Dd-AF647 during 1 h. Control cells were directly exposed to Dd without inhibitors at 37°C and untreated cells were used as negative control. Measures were done in triplicates for each cell lines and the mean ± SD is indicated. p values were determined by one-way ANOVA. ns, not significant; *$p \leq 0.05$; **$p \leq 0.01$; ***$p \leq 0.001$; ****$p < 0.0001$. (A) Effect of low temperature (4°C) and cellular ATP depletion (w/o ATP) on the internalization of Dd-AF647 (MFI). (B) Effect of endocytic inhibitors (chlorpromazine, wortmannin, and methyl-β-cyclodextrin) on the internalization of Dd-AF647 (MFI). (C) Scatterplot showing linear correlation between Dd-AF647 MFI and $\alpha_V\beta_3$ integrin MFI. The 7 cell lines were treated with 1 nM Dd-AF647 during 1 h at 37°C (without inhibitors) and then labeled with anti-$\alpha_V\beta_3$-PE monoclonal antibody. Pearson *r* coefficient of correlation and p value (two-tailed) are indicated.

at 10 nM ($p < 0.0001$, not displayed). Similar results were obtained for MFI except for granulocytes that showed a very low vector accumulation with a fold increase of 7 ± 2 at 10 nM (Figure 3A, right panel). Thus, Dd vectorizes PBMCs *ex vivo*, targeting preferentially monocytes.

Dd efficiently vectorizes AML blasts compared to ALL, targets monocytes and all subtypes of AML blasts among PBMCs, and is able to enter AML leukemic stem cells

We next analyzed the targeting of 33 leukemic patient PBMCs. Among these samples, 8 were obtained from ALL pediatric patients and 25 from AML patients, among which 84% were adult and 16% were pediatric (Table 1). As expected, Dd preferentially vectorized AML blasts compared to ALL at 1 and 10 nM, both in terms of Dd-positive cells and MFI (Figure 3B). We thus focused on AML samples (Table 2) and showed that the vector targeted blasts independently of the disease status (diagnosis versus relapse; Figures S3A and S3B), the age (pediatric versus adult patients; Figures S3C and S3D), or whether the biological sample was purified or not (Figures S3E and S3F). These data suggest the Dd as a versatile vector for AML.

Lymphocytes, granulocytes, and monocytes (LGM) were also monitored for Dd entry during vectorization of AML blasts. There was 60.5% ± 30.5% of Dd-AF647-positive cells for AML blasts at 1 nM compared to 18% ± 16% ($p < 0.0001$), 28% ± 23% ($p < 0.0001$), and 81.7% ± 19.9% ($p < 0.01$) for LGM, respectively (Figure 3C, left panel). A 10-fold concentrated dose of vector reduced these differences among populations. Quantitatively, data became statistically significant with the use of 10 nM Dd, with 313 ± 301-fold increase of MFI compared to 54 ± 47 ($p < 0.0001$), 29 ± 22 ($p < 0.0001$), and 608 ± 427 ($p < 0.0001$) for LGM (Figure 3C, right panel). It is thus noteworthy that Dd vectorizes massively AML blasts and monocytes compared to lymphocytes and granulocytes.

To go further, we analyzed the vectorization of AML subtypes according to cell morphological classification. All types of AML were vectorized with AML M4 displaying 802 ± 322-fold increase of MFI at 10 nM compared to 351 ± 263 ($p < 0.05$), 151 ± 202 ($p < 0.01$), 143 ± 154 ($p < 0.01$), and 130 ± 192 ($p < 0.001$) for secondary AML, AML M0-1-2, M3, and M5, respectively (Figure 3D). Furthermore, we analyzed Dd uptake according to the 2016-revised WHO AML classification.[4] There were no significant differences in Dd vectorization between these new AML subtypes nor for 9 AML classified with recurrent genetic abnormalities regarding *flt3*, *npm1*, and *idh1/2* classical mutations (Figures S4A and S4B). These results mean that the Dd vectorization is efficient in AML regardless of the morphological and the WHO classification.

A key feature of AML physiopathology is the presence of renewable LSCs particularly those found in granulocyte-macrophage progenitors (GMP-like LSCs).[35,36] To explore the uptake of this particular subpopulation, we treated whole marrow samples with Dd before being enriched in CD34-positive cells. Overall, a similar number of Dd-AF647-positive cells and MFI was observed for total stem cells, myeloid precursors, and GMP-like LSCs (Figure 3E).

Together, these results confirm the potential of Dd to vectorize AML blasts. Importantly, the vector is able to penetrate LSCs.

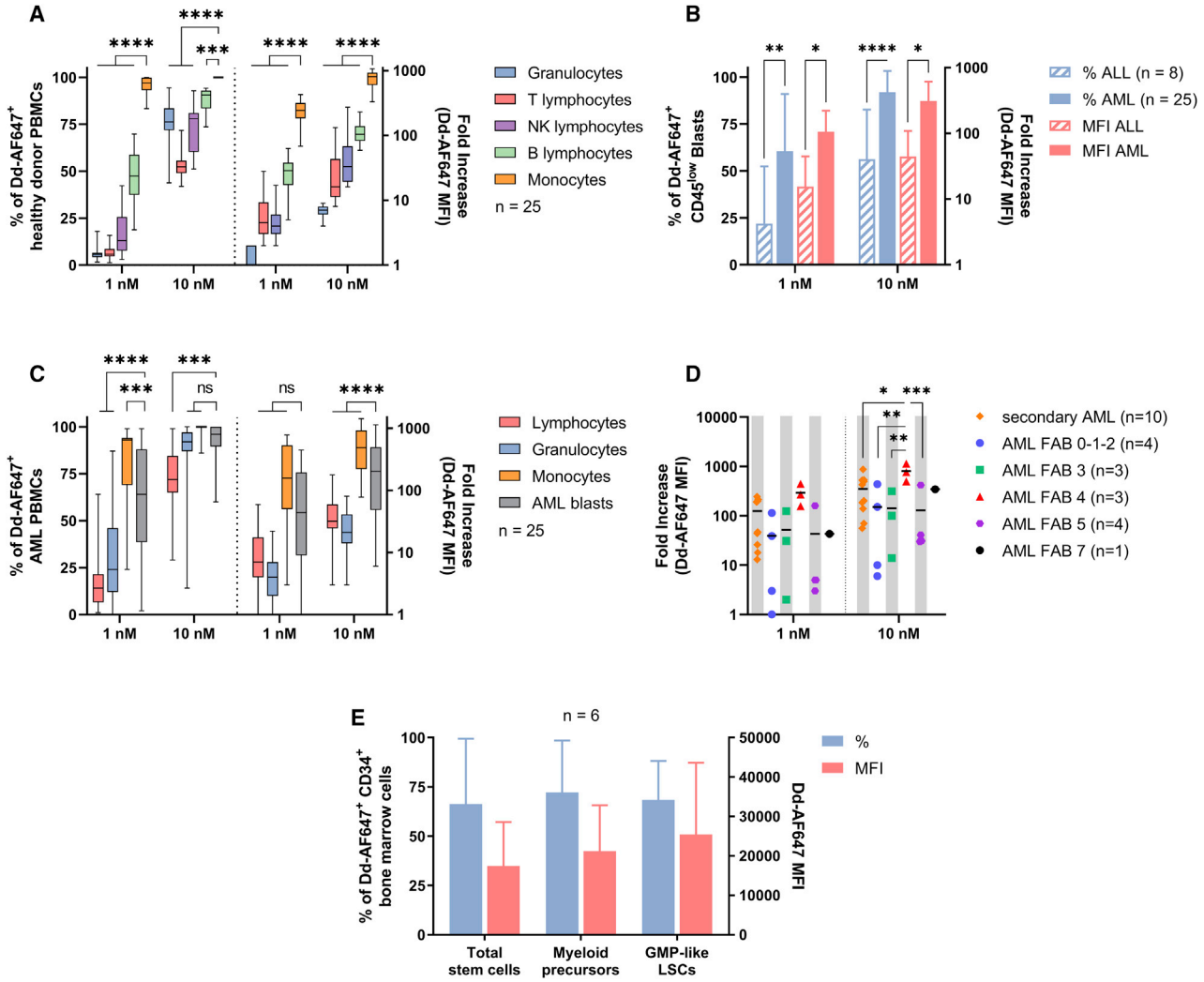

Figure 3. Dd targets preferentially monocytes among PBMCs and blasts from AML compared to ALL, addressing all AML subtypes with a higher enrichment in acute myelomonocytic leukemia, and is able to enter AML LSCs

(A–E) Healthy donor (A) and leukemic patient (B–D) PBMCs or whole bone marrow obtained from AML patients (E) were incubated with Dd-AF647 during 2 h. Cells positive (%) for Dd-AF647 (A, C, left panel; B, E, in blue). Fold increase in Dd-AF647 MFI (A, C, right panel; B, in red; D) or Dd-AF647 MFI (E in red). Results represent the mean ± SD and the corresponding number of samples is indicated. p values were determined by Student t tests (B) or two-way ANOVA (A, C, and D). *$p \leq 0.05$; **$p \leq 0.01$; ***$p \leq 0.001$; ****$p < 0.0001$. (A) Dd penetration within subpopulations of healthy donor PBMCs. Min/Max values (external lines) are also indicated. Cells were identified as follows: $CD45^+$ $CD66b^+$ for remaining granulocytes after PBMCs purification (blue), $CD45^+$ $CD3^+$ for T lymphocytes (red), $CD45^+$ $CD3^-$ $CD19^-$ $CD56^+$ for NK lymphocytes (purple), $CD45^+$ $CD19^+$ for B lymphocytes (green), and $CD45^+$ $CD33^+$ $CD14^+$ for monocytes (orange). (B) Vectorization of SSC^{low} $CD45^{low}$ blasts from ALL (n = 8) versus AML (n = 25). (C) Dd penetration within subpopulations of 25 AML PBMCs. Min/Max values (external lines) are also indicated. Subpopulations were identified as follows: SSC^{low} $CD45^{high}$ $CD3^+$ and $CD19^+$ and $CD56^+$ for lymphocytes (red), SSC^{high} $CD45^+$ $CD66b^+$ for remaining granulocytes after PBMCs purification (blue), SSC^{int} $CD45^+$ $CD33^+$ $CD14^+$ for monocytes (orange), and SSC^{low} $CD45^{low}$ distinct population for AML blasts (gray). (D) Vectorization of SSC^{low} $CD45^{low}$ AML blasts according to the morphological French-American-British (FAB) classification (n = 25). Single patient values are displayed, and the mean is indicated by a black line. Secondary AML represent AML contracted after a myelodysplastic syndrome, myeloproliferative syndrome, chronic myelomonocytic leukemia, and chemotherapy. FAB M0-1-2 define undifferentiated AML or with minimal differentiation/maturation; FAB M3, acute promyelocytic leukemia; FAB M4, acute myelomonocytic leukemia; FAB M5, acute monocytic leukemia and FAB M7, acute megakaryoblastic leukemia. (E) Vectorization of stem cells with 1 nM Dd-AF647. Cells were enriched for CD34 expression after Dd incubation using magnetic sorting. Total stem cells, $CD34^+$; Myeloid precursors, $CD34^+$ $CD33^+$; and GMP-like LSCs, Lin- $CD34^+$ $CD38^+$ $CD123^+$ $CD45RA^+$.

Dd reaches peripheral monocytes and bone marrow precursors *in vivo*

Finally, an *in vivo* biodistribution study was conducted to confirm Dd vectorization properties. Mice were i.v. injected with Dd-AF647 and sacrificed at 1-, 5-, and 12-h post-injection. *Ex vivo* fluorescence imaging was performed on isolated organs (Figure 4A). An important uptake was observed in the kidney at 1 and 5 h and in the liver at the 3 time points while only a weak

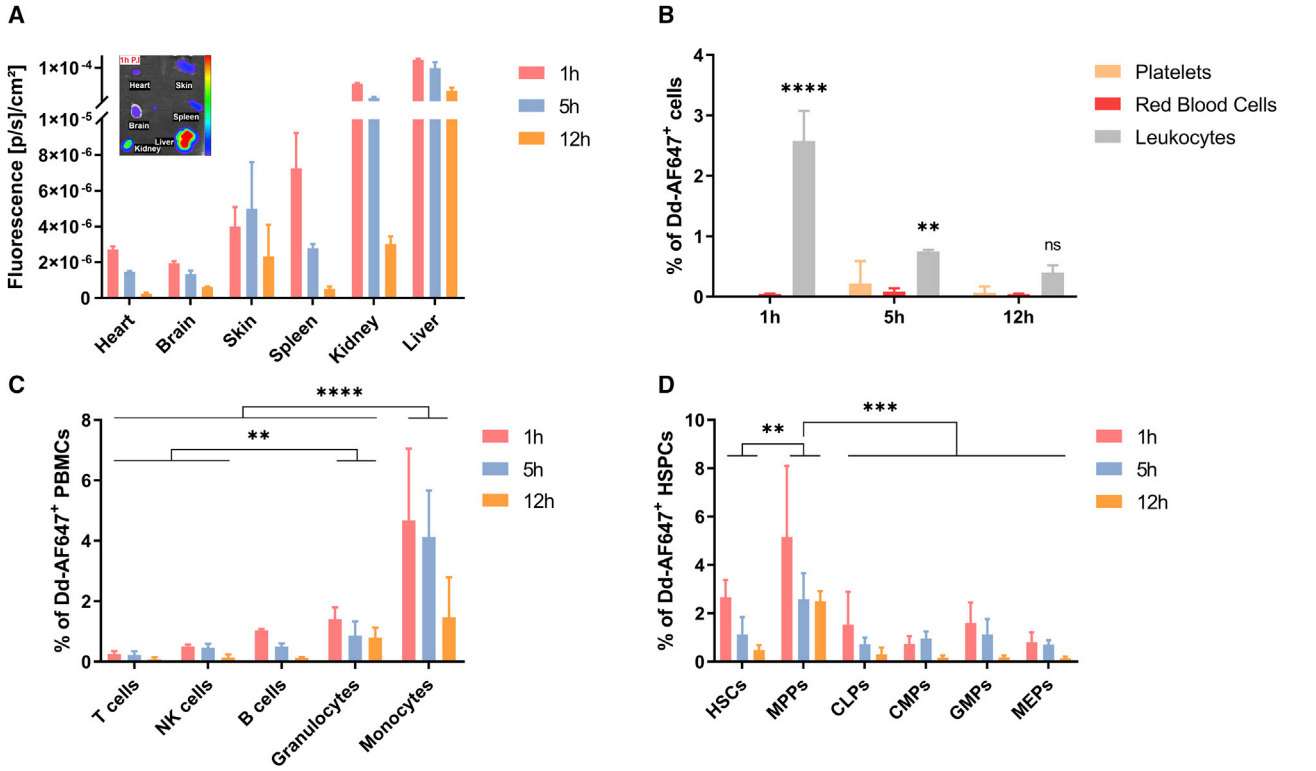

Figure 4. Dd demonstrates limited vector spreading outside the bloodstream and reach peripheral monocytes and bone marrow precursors *in vivo*.
Mice were injected i.v. with 100 µg Dd-AF647 in 200 µL of PBS (n = 9) or with 200 µL of PBS alone (n = 3). Three mice were sacrificed at 1-, 5-, and 12-h post-injection (p.i.). Organs and cells from PBS-injected mice were used as vehicle control. Results represent the mean (n = 3) ± SD. p values were determined by Student t tests (B) or two-way ANOVA (C and D). *$p \leq 0.05$; **$p \leq 0.01$; ***$p \leq 0.001$; ****$p < 0.0001$. (A) 2D fluorescence imaging performed *ex vivo* on isolated organs, displayed in [photon/sec]/cm^2. Insert: a sample image of a mouse sacrificed 1 h p.i. (B) Principal blood constituents positive (%) for Dd-AF647. Platelets, red blood cells, and leukocytes were gated by their specific expression of CD41, TER-119 (Ly-76), and CD45, respectively. (C) Lymphoid and myeloid lineages positive (%) for Dd-AF647. Subpopulations were identified with the following markers: CD45^{high} and CD3$^+$ for T lymphocytes or CD335$^+$ (NKp46) for NK lymphocytes or CD19$^+$ for B lymphocytes, CD45$^+$ CD11c- MHCII- GR1$^+$ (Ly-6G) for granulocytes, and CD45$^+$ CD11c$^{low/neg}$ MHCII$^+$ F4/80$^+$ (Ly-71) for monocytes. (D) Stem cells and early precursors positive (%) for Dd-AF647. Subpopulations were identified as follows: Lin- Sca1$^+$ c-Kit$^+$ CD135- CD34$^+$ for hematopoietic stem cells (HSCs), Lin- Sca1$^+$ c-Kit$^+$ CD135$^+$ CD34$^+$ for multipotent progenitors (MPPs), Lin$^-$ CD127$^+$ Sca1$^+$ c-Kit$^+$ for common lymphoid progenitors (CLPs), Lin$^-$ CD127$^-$ Sca1$^-$ c-Kit$^+$ CD16/32- CD34$^+$ for common myeloid progenitors (CMPs), Lin$^-$ CD127$^-$ Sca1$^-$ c-Kit$^+$ CD16/32$^+$ CD34$^+$ for granulocyte-monocyte progenitors (GMPs), and Lin$^-$ CD127$^-$ Sca1$^-$ c-Kit$^+$ CD16/32$^-$ CD34$^-$ for megakaryocyte-erythrocyte progenitors (MEPs).

signal arose from other organs including heart, brain, skin, and spleen.

Additionally, peripheral blood and bone marrow were analyzed. Although we used a small injected amount of Dd, a qualitative analysis of targeted cells could be performed. Leukocytes were the major vectorized population with regard to platelets and RBCs at 1 h and the signal decreased rapidly over 12 h (Figure 4B). The study of leukocytes subsets revealed that monocytes were also preferentially targeted *in vivo* (Figure 4C).

Bone marrow hematopoietic stem and progenitor cells (HSPCs) showed interesting results (Figure 4D). The best-targeted population was the multipotent progenitors (MPPs) with a 3 time points-mean of 3.42% ± 1.51% of vector-positive cells, compared to 0.85% ± 0.63%, 0.62% ± 0.41%, 0.97% ± 0.72%, and 0.55% ± 0.36% for the common-lymphoid progenitors (CLPs), the common-myeloid progenitors (CMPs), the GMPs, and the megakaryocyte-erythrocyte progenitors (MEPs), respectively ($p < 0.001$). HSCs displayed a mean of 1.43% ± 1.13% of Dd-AF647-positive cells that was lower than for MPPs ($p < 0.01$). Comparisons between CLPs, CMPs, GMPs, and MEPs were difficult as these populations showed similar but lower percentage of Dd penetration. Thus, all bone-marrow-resident HSPCs were reached by Dd upon i.v. injection with MPPs accumulating more Dd than other cells.

Taken together, these results recapitulate *ex vivo* observations and further demonstrate Dd ability to vectorize peripheral leukocytes *in vivo*, especially monocytes. Importantly, Dd reaches the bone marrow where it vectorizes progenitors, which is an important property for AML treatment delivery and targeting of LSCs.

DISCUSSION

The targeted delivery of AML cells is crucial for the improvement of chemotherapy tolerability by reducing unspecific off-target effects

Table 1. Description of acute lymphoid leukemia and acute myeloid leukemia patient population

	ALL (n, %)	AML (n, %)
Number of samples	8 (16)	25 (84)
Sex (male %)	62.5	68
Age at diagnosis		
<2	0	2 (8)
2–10	5 (62.5)	1 (4)
10–18	3 (37.5)	1 (4)
18–60	N/A	9 (36)
>60	N/A	12 (48)

ALL, acute lymphoid leukemia; AML, acute myeloid leukemia

and subsequent acute and chronic toxicities mediated by intensive treatment.[5,6,8] Furthermore, myeloid delivery systems are scarce and urgently needed for the avenue of new therapies. In this study, we fully evaluated the use of a non-infectious VLP as a vector to target AML cells since it presents a natural affinity for leukocytes.[30] Dd highlights several advantageous properties to represent an interesting delivery system in AML:

The vector is only composed of Ad3 Pbs, and 12 copies are sufficient to trigger the assembly of a dodecahedral VLP that is massively produced upon recombinant expression.[23,24] In addition, the vector is easily purifiable using size-exclusion followed by anion-exchange chromatography. Hence, it could be efficiently manufactured. Comparatively to the virus of origin, Dd is devoid of genome, hexon, and fiber proteins, and thus simpler and non-infectious. Although pre-existing or *de novo* generations of neutralizing anti-Ad3 antibodies could mitigate efficient drug vectorization, it has been shown that the hexon was the main target of pre-existing antibodies as well as adenovirus specific $CD4^+$ and $CD8^+$ T cells.[14,37,38] Moreover, Zochowska et al.[29] showed only a slow and moderate build-up of anti-Dd antibodies following 5 i.v. injections in rats. This suggest a limited vector neutralization risk at therapy initiation and over time.

The Ad3 infects epithelial and hematopoietic cells using macropinocytosis as a major entry pathway.[39] Comparatively, the endocytic targeting of Dd mainly involved energy-dependent CME in tested leukemic cells. This behavior might thus be related to the simpler vector composition of only Pbs. The use of a fiberless Dd also restrains undesired cell tropism by reducing the number of attachment receptors.[16–18] In this sense, it has been shown that the Ad3 enters platelets and granulocytes using fiber-mediated binding of desmoglein-2[17] while in this study, fiberless Dd showed only a slight internalization in these cells. Importantly, Dd keeps the ability to trigger-specific endocytosis through the interaction of Pb RGD motifs with $\alpha_V\beta_3$ integrins.[20,25] This feature confers, at least, a relative selectivity toward α_V integrins expression and especially $\alpha_V\beta_3$ such as for highly expressing leukemic cell lines, as well as monocytes,[40,41] AML cells,[42–44] and bone marrow progenitors[45–47] that were efficiently targeted. However, dedicated mechanistic studies could deeper characterized this $\alpha_V\beta_3$-correlated, CME-mediated endocytosis in AML cells, since partial entrapment in lysosomes has been described and that could mitigate vectorized molecules effectiveness.[27] Besides, it was shown that Dd preferentially penetrates leukocytes than platelets or RBCs in healthy donor blood.[30] That distinct vectorization efficiency was confirmed and we further revealed monocytes, as well as AML blasts to be better vectorized than ALL blasts, lymphocytes (T, B, and NK) and granulocytes. Additionally, Dd slightly spread outside the bloodstream with most of filtration occurring in 12 h, which support a rapid clearance after i.v. injection. It is noteworthy that Dd entered the heart weakly, which is promising for AML to circumvent the cardiotoxicity induced by anthracyclines.[6] The limited vector spreading is of great importance to allow optimal leukocytes targeting while reducing systemic toxicity. Altogether, these features strengthen the use of Dd to target leukemic cells compared to other carriers—with no selective cell delivery properties—such as liposomes, already evaluated in AML.[10,11]

The relevance of LSCs has been thoroughly described in AML,[36] but novel directed systems do not always evaluate the vector ability to reach these cells. The vector presented here is able to target human GMP-like LSCs *ex vivo* which, along with lymphoid-primed multipotent progenitors LSCs, coexist in 80% of patients.[35] Furthermore, upon i.v. injection in mice, the vector reached the bone marrow and HSPCs, among which MPPs were the best-vectorized. Since 10% to 15% of AML cases are characterized by a dominant population resembling MPPs,[35] that population would be potentially targeted by Dd. These features emphasize the use of Dd to target HSPCs and by extension the place where LSCs reside.

The vectorization of model leukemic cells revealed an efficient targeting at low nanomolar concentration, as well as a good intracytoplasmic maintenance of the fluorescent cargo. These points are of importance since intensive chemotherapy treatment induces efflux-mediated multidrug resistance (MDR) mechanisms that greatly contribute to AML relapses.[48] Of note, the vectorization of AML blasts obtained from relapsed patients was as effective as the vectorization of patient blasts at diagnosis. Thus, the enhanced retaining time of cargo provided with low concentration of Dd could circumvent those hurdles, similarly to doxorubicin in the context of human MDR sarcoma cells.[30] Since our data also indicate a moderate toxicity of Dd, its utilization as a vector might be safe *in vivo*. Hence, Dd and chemotherapy could be associated to enhance the effect of free therapeutic form, thereby reducing off-targets and side effects. Using this strategy, the effective cytotoxic concentration of bleomycin delivered with Dd to human cervical cancer cells was 100 times lower than that of free drug.[28] Thus, the vector is effective from very low molecular concentrations, supporting its use as an efficient enhancer for therapeutics in AML cells also via improvement of cell retention while cytotoxicity of Dd remains acceptable.

In conclusion, these results highlight promising features of Dd vector for myeloid and monocytes cell delivery applications, as well as for

Table 2. Classification of pediatric and adult AML patient population

	Pediatric (n, %)	Adult (n, %)
AML at		
Diagnosis	4 (100)	21 (71)
Relapsing	0	6 (29)
FAB classification		
M0	1 (25)	5 (24)
M1	0	2 (10)
M2	1 (25)	7 (33)
M3	0	1 (5)
M4	0	3 (14)
M5	1 (25)	3 (14)
M6	0	0
M7	1 (25)	0
WHO classification		
AML with recurrent genetic abnormalities	2 (50)	7 (33)
flt3	1 (25)	3 (14)
npm1	0	2 (10)
idh1/2	0	2 (10)
Others	1 (25)	0
AML with myelodysplasia related changes	0	8 (38)
therapy-related AML	1 (25)	0
AML not otherwise specified	1 (25)	6 (25)

AML therapy-aiming at targeting preferentially blasts and HSPCs. Further studies should now consider a therapeutic form of Dd such as Dd bearing doxorubicin and assess its full potential in AML engrafted mice models in comparison to free-drug doxorubicin or another reference therapy.

MATERIALS AND METHODS

Dd labeling

Dd was conjugated to Alexa Fluor 647 (Dd-AF647) using AF647 Protein Labeling Kit (Molecular Probes) and the structure was verified by nanoparticle tracking analysis on a NanoSight NS300 (Malvern Panalytical).

Dd cell vectorization

Leukemic cell lines, PBMCs, bone marrow mononuclear cells and whole blood/bone marrow were incubated with 0.01 to 10 nM Dd-AF647 for up to 7 days at 37°C. Untreated cells or whole blood/bone marrow were used as controls. After incubation, purified cells were treated with 0.5% Trypsin-EDTA (GIBCO) during 5 min at 37°C to remove surface-bound Dd. For LSCs vectorization, CD34 enrichment was performed using CD34 MicroBeads kit (autoMACS Pro, Miltenyi Biotech).

Cytotoxicity assays

The Dd toxicity was assessed on cell lines using a metabolic assessment of cell viability by a chromogenic assay. Cells were quantified using CellTiter 96 Aqueous One Solution Cell Proliferation Assay (Promega) on a Varioskan Flash (Thermo Scientific). Doxorubicin (Accord) was used as a positive control for cell death.

Confocal microscopy

Cells were treated with PBS or 10 nM Dd-AF647 for 2 h at 37°C. After incubation, cells were fixed with 1× FACS lysing solution (BD Biosciences). Nuclei were stained with DAPI (1:3,000; Sigma) and membranes with Alexa Fluor 555-conjugated wheat germ agglutinin (WGA; 1:200; Invitrogen) during 10 min at room temperature. Images were acquired after sequential laser excitation using an LSM 710 NLO laser-scanning microscope (Zeiss) onto optical sectioning of 1 μm and analyzed with ImageJ software.

Drug treatment

Cells were pre-incubated during 1 h prior to Dd addition in PBS containing the following drugs: 100 nM wortmannin, 30 μM chlorpromazine hydrochloride, 500 μM MBCD, 10 mM 2-deoxy-D-glucose, and 10 mM sodium azide (Sigma).

Flow cytometry

Human and mouse antibodies were purchased from BD Biosciences. In all experiments, cells were selected by a viability labeling using Zombie Aqua Fixable Viability Kit (BioLegend). The percentage of Dd-AF647 positive cells and AF647 MFI were measured for each population. The threshold percent gate was set up by cell type for background fluorescence of untreated cells. The MFI of Dd-AF647-treated cells was compared to control by dividing (fold increase) or subtracting the MFI of the corresponding untreated cells. For measurement of $\alpha_V\beta_3$ integrin expression, cells were labeled with anti-$\alpha_V\beta_3$-PE monoclonal antibody. Data were acquired on FACS Canto II and FACS LSR II (Beckton Dickinson) and analyzed with FlowJo V10 software.

In vivo biodistribution in blood and bone marrow

The project was authorized by the French ministry of research with the permit number: APAFIS#18922-2019013112124432v4. Twelve 5-week-old C57Black6 female mice were purchased (Janvier Laboratory) and housed for 1 week before the day of experiment. Mice were injected in the tail vein with 100 μg Dd-AF647 in 200 μL of PBS (n = 9) or with 200 μL of PBS alone (n = 3). Three mice were anesthetized per time point at 1, 5, and 12 h post-injection, 500 μL of blood were collected and mice were sacrificed for organs and bone marrow sampling.[49]

Statistics

Data are reported as the mean values ± standard deviation (SD). Student t test was used in univariate analysis and Pearson *r* coefficient was calculated for correlation. One-way or two-way ANOVA tests were performed for multivariate analysis, and p values were conservatively adjusted for multiple comparisons using a Bonferroni correction. p value <0.05 was considered significant and the abbreviations were: n.s., not significant; *$p \leq 0.05$; **$p \leq 0.01$; ***$p \leq 0.001$; ****$p < 0.0001$. Statistics were calculated using GraphPad Prism V7 software.

SUPPLEMENTAL INFORMATION

Supplemental Information can be found online at https://doi.org/10.1016/j.omtm.2020.11.009.

ACKNOWLEDGMENTS

This work was funded by Société Française de lutte contre les Cancers et les leucémies de l'Enfant et de l'adolescent, La Ligue contre le Cancer 38, Association Grenobloise pour le Développement d'Etudes et de Recherche en Médecine Infantile, Association Espoir, GEFLUC Grenoble Dauphiné-Savoie, and IDEX University Grenoble Alpes. The authors thanks Sylvie Berthier of the Institute of Biology and Pathology (Grenoble) for access to and technical assistance with flow cytometers; Alexei Grichine and Mylène Pezet of the Institute for Advanced Biosciences (Grenoble) for technical assistance with confocal microscopes and flow cytometers; Gautier Szymancki, Claire Vettier, Christine Lefebvre, and the technicians of the Laboratory of Cellular Hematology (Grenoble) for providing patient samples; Pascal Fender of the Institut de Biologie Structurale (IBS, Grenoble) for helpful advice and discussions on the adenoviral Dd; Marta Jedynak and Ewa Szolajska of the Institute of Biochemistry and Biophysics (Warsaw, Poland) for materials and discussions on the adenoviral Dd; Karine Laulagnier from Remy Sadoul group of the Grenoble Institute of Neuroscience (Grenoble) for access to Nanosight and advice on particle analysis; and Daphna Fenel and Guy Schoehn of the electron microscopy (EM) IBS platform (Grenoble). This work used the EM facilities at the Grenoble Instruct-ERIC Center (ISBG; UMS 3518 CNRS CEA-UJF-EMBL) with support from the French Infrastructure for Integrated Structural Biology (FRISBI; ANR-10-INSB-05-02) and the Grenoble Alliance for Integrated Structural Cell Biology (GRAL; ANR-10-LABX-49-01) within the Grenoble Partnership for Structural Biology. The IBS EM platform is supported by the Rhône-Alpes Region, the Fonds Feder, the Fondation pour la Recherche Médicale, and GIS-IBiSA.

AUTHOR CONTRIBUTIONS

Conceptualization, B.C., D.H., D.L., and J.C.; Methodology, B.C., D.H., and J.C.; Investigation, B.C., G.S., D.H., and M.G.; Validation, Formal Analysis, Visualization and Writing – Original Draft, B.C.; Writing – Review & Editing, B.C., D.H., V.J., D.L., J.C., P.M., and D.P.; Funding Acquisition, D.L., J.C., and D.P.; Resources, J.C., P.M., and D.P.; Supervision, B.C., P.M., and D.P.

DECLARATION OF INTERESTS

The authors declare no competing interests.

REFERENCES

1. Rasche, M., Zimmermann, M., Borschel, L., Bourquin, J.-P., Dworzak, M., Klingebiel, T., Lehrnbecher, T., Creutzig, U., Klusmann, J.-H., and Reinhardt, D. (2018). Successes and challenges in the treatment of pediatric acute myeloid leukemia: a retrospective analysis of the AML-BFM trials from 1987 to 2012. Leukemia *32*, 2167–2177.

2. Creutzig, U., van den Heuvel-Eibrink, M.M., Gibson, B., Dworzak, M.N., Adachi, S., de Bont, E., Harbott, J., Hasle, H., Johnston, D., Kinoshita, A., et al.; AML Committee of the International BFM Study Group (2012). Diagnosis and management of acute myeloid leukemia in children and adolescents: recommendations from an international expert panel. Blood *120*, 3187–3205.

3. Döhner, H., Estey, E.H., Amadori, S., Appelbaum, F.R., Büchner, T., Burnett, A.K., Dombret, H., Fenaux, P., Grimwade, D., Larson, R.A., et al.; European LeukemiaNet (2010). Diagnosis and management of acute myeloid leukemia in adults: recommendations from an international expert panel, on behalf of the European LeukemiaNet. Blood *115*, 453–474.

4. Arber, D.A., Orazi, A., Hasserjian, R., Thiele, J., Borowitz, M.J., Le Beau, M.M., Bloomfield, C.D., Cazzola, M., and Vardiman, J.W. (2016). The 2016 revision to the World Health Organization classification of myeloid neoplasms and acute leukemia. Blood *127*, 2391–2405.

5. Döhner, H., Weisdorf, D.J., and Bloomfield, C.D. (2015). Acute Myeloid Leukemia. N. Engl. J. Med. *373*, 1136–1152.

6. McGowan, J.V., Chung, R., Maulik, A., Piotrowska, I., Walker, J.M., and Yellon, D.M. (2017). Anthracycline Chemotherapy and Cardiotoxicity. Cardiovasc. Drugs Ther. *31*, 63–75.

7. Leung, W., Hudson, M.M., Strickland, D.K., Phipps, S., Srivastava, D.K., Ribeiro, R.C., Rubnitz, J.E., Sandlund, J.T., Kun, L.E., Bowman, L.C., et al. (2000). Late effects of treatment in survivors of childhood acute myeloid leukemia. J. Clin. Oncol. *18*, 3273–3279.

8. Briot, T., Roger, E., Thépot, S., and Lagarce, F. (2018). Advances in treatment formulations for acute myeloid leukemia. Drug Discov. Today *23*, 1936–1949.

9. Torchilin, V.P. (2014). Multifunctional, stimuli-sensitive nanoparticulate systems for drug delivery. Nat. Rev. Drug Discov. *13*, 813–827.

10. Krauss, A.C., Gao, X., Li, L., Manning, M.L., Patel, P., Fu, W., Janoria, K.G., Gieser, G., Bateman, D.A., Przepiorka, D., et al. (2019). FDA Approval Summary: (Daunorubicin and Cytarabine) Liposome for Injection for the Treatment of Adults with High-Risk Acute Myeloid Leukemia. Clin. Cancer Res. *25*, 2685–2690.

11. European public assessment reports (2018). Vyxeos liposomal (previously known as Vyxeos). European Medicines Agency, https://www.ema.europa.eu/en/medicines/human/EPAR/vyxeos-liposomal.

12. Yoo, J.-W., Irvine, D.J., Discher, D.E., and Mitragotri, S. (2011). Bio-inspired, bioengineered and biomimetic drug delivery carriers. Nat. Rev. Drug Discov. *10*, 521–535.

13. Koudelka, K.J., Pitek, A.S., Manchester, M., and Steinmetz, N.F. (2015). Virus-Based Nanoparticles as Versatile Nanomachines. Annu. Rev. Virol. *2*, 379–401.

14. Sumida, S.M., Truitt, D.M., Lemckert, A.A.C., Vogels, R., Custers, J.H.H.V., Addo, M.M., Lockman, S., Peter, T., Peyerl, F.W., Kishko, M.G., et al. (2005). Neutralizing antibodies to adenovirus serotype 5 vaccine vectors are directed primarily against the adenovirus hexon protein. J. Immunol. *174*, 7179–7185.

15. Fausther-Bovendo, H., and Kobinger, G.P. (2014). Pre-existing immunity against Ad vectors: humoral, cellular, and innate response, what's important? Hum. Vaccin. Immunother. *10*, 2875–2884.

16. Gaggar, A., Shayakhmetov, D.M., and Lieber, A. (2003). CD46 is a cellular receptor for group B adenoviruses. Nat. Med. *9*, 1408–1412.

17. Wang, H., Li, Z.-Y., Liu, Y., Persson, J., Beyer, I., Möller, T., Koyuncu, D., Drescher, M.R., Strauss, R., Zhang, X.-B., et al. (2011). Desmoglein 2 is a receptor for adenovirus serotypes 3, 7, 11 and 14. Nat. Med. *17*, 96–104.

18. Short, J.J., Pereboev, A.V., Kawakami, Y., Vasu, C., Holterman, M.J., and Curiel, D.T. (2004). Adenovirus serotype 3 utilizes CD80 (B7.1) and CD86 (B7.2) as cellular attachment receptors. Virology *322*, 349–359.

19. Wickham, T.J., Mathias, P., Cheresh, D.A., and Nemerow, G.R. (1993). Integrins alpha v beta 3 and alpha v beta 5 promote adenovirus internalization but not virus attachment. Cell *73*, 309–319.

20. Cuzange, A., Chroboczek, J., and Jacrot, B. (1994). The penton base of human adenovirus type 3 has the RGD motif. Gene *146*, 257–259.

21. Xiong, J.-P., Stehle, T., Zhang, R., Joachimiak, A., Frech, M., Goodman, S.L., and Arnaout, M.A. (2002). Crystal structure of the extracellular segment of integrin alpha Vbeta3 in complex with an Arg-Gly-Asp ligand. Science *296*, 151–155.

22. Fender, P., Boussaid, A., Mezin, P., and Chroboczek, J. (2005). Synthesis, cellular localization, and quantification of penton-dodecahedron in serotype 3 adenovirus-infected cells. Virology *340*, 167–173.

23. Fender, P., Ruigrok, R.W.H., Gout, E., Buffet, S., and Chroboczek, J. (1997). Adenovirus dodecahedron, a new vector for human gene transfer. Nat. Biotechnol. *15*, 52–56.

24. Szolajska, E., Burmeister, W.P., Zochowska, M., Nerlo, B., Andreev, I., Schoehn, G., Andrieu, J.-P., Fender, P., Naskalska, A., Zubieta, C., et al. (2012). The structural basis for the integrity of adenovirus Ad3 dodecahedron. PLoS ONE *7*, e46075.

25. Fender, P., Schoehn, G., Perron-Sierra, F., Tucker, G.C., and Lortat-Jacob, H. (2008). Adenovirus dodecahedron cell attachment and entry are mediated by heparan sulfate and integrins and vary along the cell cycle. Virology *371*, 155–164.

26. Garcel, A., Gout, E., Timmins, J., Chroboczek, J., and Fender, P. (2006). Protein transduction into human cells by adenovirus dodecahedron using WW domains as universal adaptors. J. Gene Med. *8*, 524–531.

27. Sumarheni, G.B., and Fender, P. (2016). The Use of Adenovirus Dodecahedron in the Delivery of an Enzymatic Activity in the Cell. Biotechnol. Res. Int. *2016*, 5030589.

28. Zochowska, M., Paca, A., Schoehn, G., Andrieu, J.-P., Chroboczek, J., Dublet, B., and Szolajska, E. (2009). Adenovirus dodecahedron, as a drug delivery vector. PLoS ONE *4*, e5569.

29. Zochowska, M., Piguet, A.-C., Jemielity, J., Kowalska, J., Szolajska, E., Dufour, J.-F., and Chroboczek, J. (2015). Virus-like particle-mediated intracellular delivery of mRNA cap analog with in vivo activity against hepatocellular carcinoma. Nanomedicine (Lond.) *11*, 67–76.

30. Jedynak, M., Laurin, D., Dolega, P., Podsiadla-Bialoskorska, M., Szurgot, I., Chroboczek, J., and Szolajska, E. (2018). Leukocytes and drug-resistant cancer cells are targets for intracellular delivery by adenoviral dodecahedron. Nanomedicine (Lond.) *14*, 1853–1865.

31. Araki, N., Johnson, M.T., and Swanson, J.A. (1996). A role for phosphoinositide 3-kinase in the completion of macropinocytosis and phagocytosis by macrophages. J. Cell Biol. *135*, 1249–1260.

32. Nabi, I.R., and Le, P.U. (2003). Caveolae/raft-dependent endocytosis. J. Cell Biol. *161*, 673–677.

33. Wang, L.H., Rothberg, K.G., and Anderson, R.G. (1993). Mis-assembly of clathrin lattices on endosomes reveals a regulatory switch for coated pit formation. J. Cell Biol. *123*, 1107–1117.

34. Vivès, R.R., Lortat-Jacob, H., Chroboczek, J., and Fender, P. (2004). Heparan sulfate proteoglycan mediates the selective attachment and internalization of serotype 3 human adenovirus dodecahedron. Virology *321*, 332–340.

35. Goardon, N., Marchi, E., Atzberger, A., Quek, L., Schuh, A., Soneji, S., Woll, P., Mead, A., Alford, K.A., Rout, R., et al. (2011). Coexistence of LMPP-like and GMP-like leukemia stem cells in acute myeloid leukemia. Cancer Cell *19*, 138–152.

36. Thomas, D., and Majeti, R. (2017). Biology and relevance of human acute myeloid leukemia stem cells. Blood *129*, 1577–1585.

37. Serangeli, C., Bicanic, O., Scheible, M.H., Wernet, D., Lang, P., Rammensee, H.-G., Stevanovic, S., Handgretinger, R., and Feuchtinger, T. (2010). Ex vivo detection of adenovirus specific CD4+ T-cell responses to HLA-DR-epitopes of the Hexon protein show a contracted specificity of T(HELPER) cells following stem cell transplantation. Virology *397*, 277–284.

38. Leen, A.M., Christin, A., Khalil, M., Weiss, H., Gee, A.P., Brenner, M.K., Heslop, H.E., Rooney, C.M., and Bollard, C.M. (2008). Identification of hexon-specific CD4 and CD8 T-cell epitopes for vaccine and immunotherapy. J. Virol. *82*, 546–554.

39. Amstutz, B., Gastaldelli, M., Kälin, S., Imelli, N., Boucke, K., Wandeler, E., Mercer, J., Hemmi, S., and Greber, U.F. (2008). Subversion of CtBP1-controlled macropinocytosis by human adenovirus serotype 3. EMBO J. *27*, 956–969.

40. Weerasinghe, D., McHugh, K.P., Ross, F.P., Brown, E.J., Gisler, R.H., and Imhof, B.A. (1998). A role for the alphavbeta3 integrin in the transmigration of monocytes. J. Cell Biol. *142*, 595–607.

41. Brilha, S., Wysoczanski, R., Whittington, A.M., Friedland, J.S., and Porter, J.C. (2017). Monocyte Adhesion, Migration, and Extracellular Matrix Breakdown Are Regulated by Integrin αVβ3 in Mycobacterium tuberculosis Infection. J.I. *199*, 982–991.

42. Al-Asadi, M.G., Brindle, G., Castellanos, M., May, S.T., Mills, K.I., Russell, N.H., Seedhouse, C.H., and Pallis, M. (2017). A molecular signature of dormancy in $CD34^{+}CD38^{-}$ acute myeloid leukaemia cells. Oncotarget *8*, 111405–111418.

43. Miller, P.G., Al-Shahrour, F., Hartwell, K.A., Chu, L.P., Järås, M., Puram, R.V., Puissant, A., Callahan, K.P., Ashton, J., McConkey, M.E., et al. (2013). In Vivo RNAi screening identifies a leukemia-specific dependence on integrin beta 3 signaling. Cancer Cell *24*, 45–58.

44. Johansen, S., Brenner, A., Bartaula-Brevik, S., Reikvam, H., and Bruserud, Ø. (2018). The Possible Importance of β3 Integrins for Leukemogenesis and Chemoresistance in Acute Myeloid Leukemia. IJMS *19*, 251.

45. Umemoto, T., Matsuzaki, Y., Shiratsuchi, Y., Hashimoto, M., Yoshimoto, T., Nakamura-Ishizu, A., Petrich, B., Yamato, M., and Suda, T. (2017). Integrin αvβ3 enhances the suppressive effect of interferon-γ on hematopoietic stem cells. EMBO J. *36*, 2390–2403.

46. Kräter, M., Jacobi, A., Otto, O., Tietze, S., Müller, K., Poitz, D.M., Palm, S., Zinna, V.M., Biehain, U., Wobus, M., et al. (2017). Bone marrow niche-mimetics modulate HSPC function via integrin signaling. Sci. Rep. *7*, 2549.

47. Wang, J., Liu, Z., Zhang, S., Wang, X., Bai, H., Xie, M., Dong, F., and Ema, H. (2019). Lineage marker expression on mouse hematopoietic stem cells. Exp. Hematol. *76*, 13–23.

48. Zhang, J., Gu, Y., and Chen, B. (2019). Mechanisms of drug resistance in acute myeloid leukemia. OncoTargets Ther. *12*, 1937–1945.

49. Liu, X., and Quan, N. (2015). Immune Cell Isolation from Mouse Femur Bone Marrow. Biol. Protoc *5*, e1631.